Ore Geology Reviews 74 (2016) 1–14

Contents lists available at ScienceDirect

Ore Geology Reviews

journal homepage: www.elsevier.com/locate/oregeorev

Geochemical, fluid inclusion and isotopic (O, H and S) constraints on the origin of Pb–Zn ± Au vein-type mineralizations in the Eastern Pontides Orogenic Belt (NE Turkey)

Enver Akaryali

Department of Geological Engineering, Gümüşhane University, 29000 Gümüşhane, Turkey

ARTICLE INFO

Article history:
Received 31 July 2015
Received in revised form 7 November 2015
Accepted 9 November 2015
Available online 11 November 2015

Keywords:
Eastern Pontides Orogenic Belt
Sulfur isotope
Epithermal vein-type
Granitic magmas

ABSTRACT

The mineralization area (Altınpınar, Torul–Gümüşhane) is situated in the Southern Zone of the Eastern Pontides Orogenic Belt (EPOB), which is one of the important metallogenic provinces in the Alpine–Himalayan belt and is intruded by the late Carboniferous granitic rocks (Gümüşhane Granitoid), an early to middle Jurassic volcano-sedimentary unit consisting mainly of basaltic–andesitic volcanic and pyroclastic rocks (Şenköy Formation) and Eocene basaltic–andesitic volcanic rocks (Alibaba Formation). The studied Pb–Zn ± Au mineralizations are related to silica veins ranging from a few millimeters to a maximum of 40 cm in thickness and are localized within fracture zones developed along the contact between the Gümüşhane Granitoid and Şenköy Formation. Silicic, sulfidic, hematitic, argillic, intense chloritic and carbonate alteration are the most common types from the fault lines toward the outer zones. Cavity filling and banded structures are widely observed. The mineral paragenesis comprises galena, sphalerite, pyrite, chalcopyrite, tennantite and quartz. Mineral chemistry studies indicate that ion exchange occurs between Zn and Fe in sphalerites, and the Zn/Cd ratio of sphalerites varies between 50.65 and 144.64. The homogenization temperatures measured from fluid inclusions vary between 170 °C and 380 °C, especially between 250 °C and 300 °C, and the wt.% NaCl eqv. salinity of ore-forming fluids is between 2.4 and 7.3 (4.7 on average), supporting an epithermal system in their origin. The values of sulfur isotopes, which are obtained from pyrite and galena minerals, range between −8.3‰ and −2.3‰, indicating that sulfur, which enables mineral formation, originates from magmatic genesis. The average formation temperature of the ore is 317 °C as determined with a sulfur isotope geothermometer. The values of oxygen and hydrogen isotopes vary between 8.5‰ and 10.2‰ and −91‰ and −73‰, respectively. With regard to the compositions of oxygen and hydrogen isotopes, fluids comprising the mineralization are formed by the mixture of magmatic water and meteoric water. This situation is supported by the fact that the increase in the homogenization temperature indicates dilution with surface water but depends on the increase in the salinity of fluid inclusions. Considering all the data, it is clear that the studied mineralization is an epithermal vein-type mineralization that is related to granitic magmas.

1. Introduction

The Pontides orogenic belt, which geographically corresponds to the northern part of Turkey and constitutes an important part of the Alpine–Himalayan system, was shaped by subduction of Tethyan oceanic lithosphere beneath the Pontide continental crust during Meso-Cenozoic time (e.g., Dewey et al., 1973; Şengör and Yılmaz, 1981; Bektaş et al., 1999; Eyuboglu et al., 2011a, 2014). However, the subduction polarity is still controversial owing to a lack of systematical geological and geochemical data. The Pontides belt is divided into three subzones as western, central and eastern Pontides from west to east. The Eastern Pontides Orogenic Belt (EPOB) is restricted by Central Pontides in the west and Lesser Caucasus in the east.

The EPOB is one of most important metallogenic provinces and hosts many types of economical ore deposits, such as volcanogenic massive sulfide (VMS), porphyry copper, skarn and epithermal vein-types. Yalçınalp (1992) asserted in his research in Güzelyayla (Maçka–Trabzon) that the Güzelyayla porphyry Cu–Mo deposit had a mesothermal characteristic and emerged between 280 and 460 °C. Turkish volcanic-hosted massive sulfide deposits are hosted by Upper Cretaceous felsic volcanics. These massive sulfide deposits are mainly Cu–Pb–Zn type owing mainly to the Cu-rich underlying rock section (Çiftçi, 2000). Tüysüz (2000) reported that silicification is restricted mainly to the ore-bearing dacites, whereas sericitic, argillic and carbonate alteration occurs widely both in dacites and overlying tuffaceous units in Murgul massive sulfide deposit (Artvin, NE Turkey). Detailed mineralogical and geochemical

E-mail address: eakaryali@gmail.com.

http://dx.doi.org/10.1016/j.oregeorev.2015.11.013
0169-1368/

studies indicate that the hydrothermal alteration zones developed wall rocks, passing away from the deposit; sericite–carbonate zone, quartz–sericite zone, Mn–Fe carbonate zone and outer propylitic zone and $\delta^{34}S$ values (+2 to +6.7‰) of sulfur minerals indicate a magmatic source for the sulfur in Midi (Gümüşhane, NE Turkey) epithermal Pb–Zn deposit (Lermi, 2003). Demir et al. (2008) determined that the formation of the Köstere (Gümüşhane) mine was related to the settlement of Torul Pluton, which is the youngest unit in the district; additionally, meteoric waters were also effective in ore formation per the average salinity values of 5.4% obtained from fluid inclusion studies. Sipahi (2011) suggested that the Fe skarn deposit at Arnastal and the skarn occurrence at Camiboğazı (Maçka–Trabzon) formed as a result of contact pyrometasomatic activities related to I-type granitoid intrusion. According to result of O, H and S isotopes coupled with mineralogical and textural data, Aslan (2011) emphasized that the Mastra (Gümüşhane) Au deposit is a low sulfidation type epithermal system. Akaryalı and Tüysüz (2013) came to the conclusion, as a result of studies conducted on the gold mineralization in the Arzular district that the gold mineralization in the Arzular (Gümüşhane) district emerged within the hydrothermal vein-type, sulfur-containing epithermal system. Demir et al. (2013) emphasized that the reason for the high silver content in the Istala deposit is (Gümüşhane) due to the input of later-stage, copper-rich, low-temperature hydrothermal fluids. Eyuboglu et al. (2014) suggested that the geodynamic setting and host rock geochemical characteristics (calc-alkaline to shoshonitic) of the eastern Pontides volcanic-hosted massive sulfide deposits are different from those of classic Kuroko-type VMS deposits and named them as "Black Sea-type Volcanogenic Massive Sulfide Deposits". In another study performed in Murgul Mine (Artvin), it has been suggested that the Murgul volcanics were derived from an enriched source, which was previously modified by subduction fluids in a geodynamic setting (Sipahi et al., 2014). On the other hand, the alteration patterns and ore formation in the Murgul (Artvin, NE Turkey) volcanic-hosted massive sulfide deposit in the northern part of the Eastern Pontides metallogenic belt were formed by hydrothermal fluids, a mixture of seawater and magmatic fluids resulting from the emplacement of late Cretaceous granitoid intrusions (Abdioğlu et al., 2015).

The Pb–Zn ± Au vein-type mineralizations are hosted by early to middle Jurassic (Lermi, 2003), late Cretaceous (Demir, 2005; Demir et al., 2008, 2013), and Eocene (Tüysüz et al., 1994; Tüysüz and Akçay, 2000; Aslan, 2011; Akaryalı, 2010; Akaryalı and Tüysüz, 2013) volcanic and pyroclastic rocks exposed in the EPOB. The studied mineralization is found in the early to middle Jurassic volcanic rocks exposed along the contact between the late Carboniferous Gümüşhane Granitoid and early to late Jurassic Şenköy Formation. Although the geological and geochemical characteristics of the rock units exposed in the mineralization field have been researched (e.g., Güner and Yazıcı, 2011; Dokuz, 2011; Eyuboglu et al., 2013a; Eyuboglu, 2015), the origin of ore deposits and hydrothermal alterations have not yet been studied.

In contrast to previous works, this study presents new geological, geochemical, fluid inclusion and stable isotope data on the origin of epithermal vein-type Altınpınar mineralization, which is exposed in

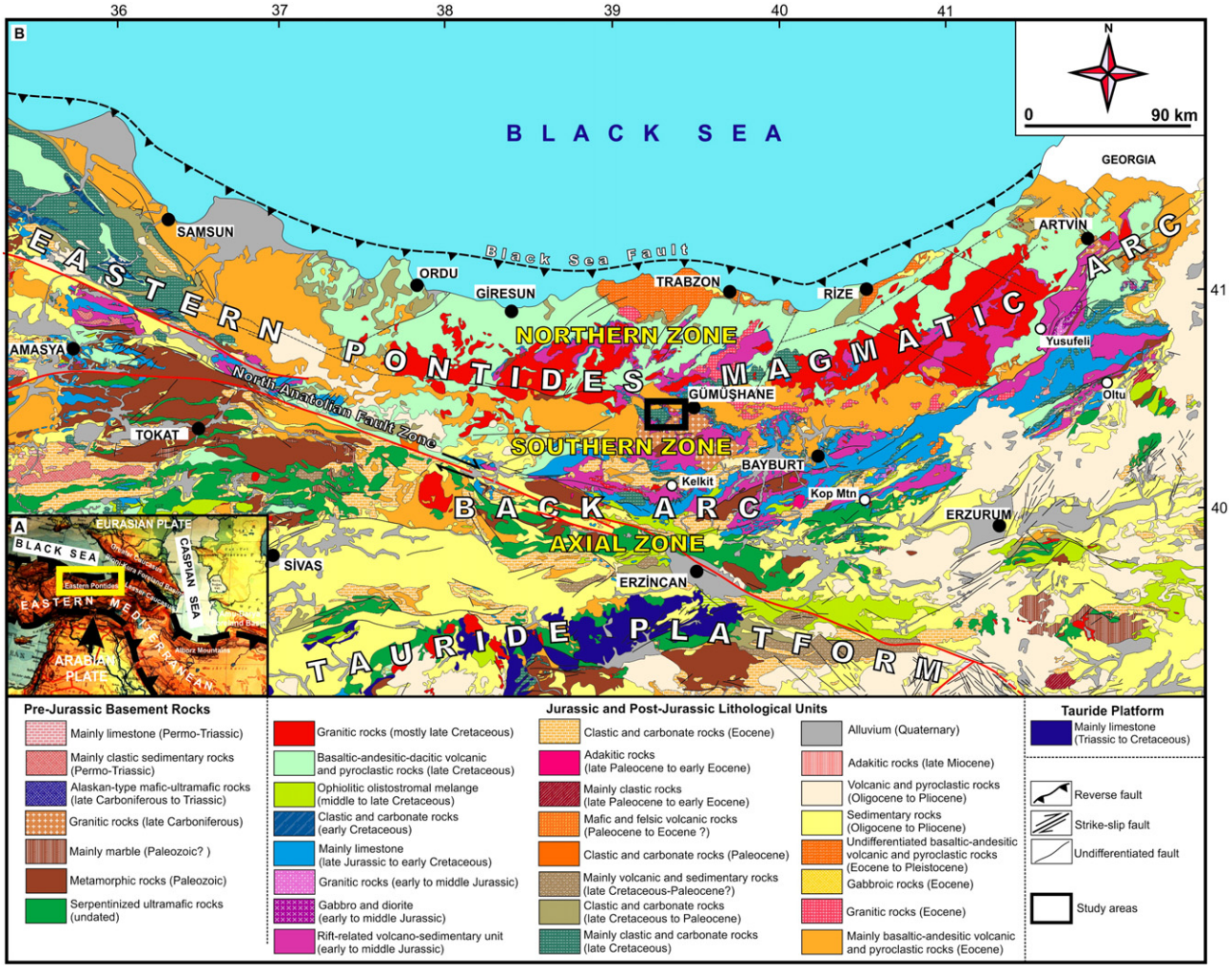

Fig. 1. Tectono-geological map showing the main lithological units and tectonic zones of the Eastern Pontides Orogenic Belt. After Eyuboglu et al. (2015a).

the Southern Zone of EPOB and its host rocks and also discusses their possible source areas and geodynamic setting considering new and old data.

2. Geological background

The EPOB can be divided into Northern, Southern and Axial subzones depending on its tectonic characteristics, lithological units and facies changes (Bektaş et al., 1995; Eyuboglu et al., 2006, 2015a, Fig. 1). The Northern Zone is generally represented by late Cretaceous and Tertiary volcanic rocks and granitic and gabbroic intrusions (e.g., Kaygusuz and Aydınçakır, 2011; Kaygusuz et al., 2014; Eyuboglu et al., 2015a). In this zone, the late Cretaceous sequence consisting mainly of basaltic–andesitic–dacitic volcanic and associated pyroclastic rocks hosts numerous economical massive sulfide deposits such as Murgul, Kutlular, Harköy, Köprübaşı and Lahanos (Fig. 2). The basement units including Paleozoic Pulur, Ağvanis and Tokat metamorphic massifs and also late Carboniferous Gümüşhane and Köse granitoids are well exposed in the Southern Zone of EPOB (e.g., Topuz et al., 2010; Dokuz, 2011). In addition to the basement rocks, late Carboniferous to Triassic Alaskan-type mafic–ultramafic intrusions (Eyuboglu et al., 2010), late Cretaceous high-K volcanic rocks (Eyuboglu, 2010) and late Paleocene–early Eocene adakitic rocks (Topuz et al., 2005; Karslı et al., 2010; Eyuboglu et al., 2011a) are the most common rock units in the Southern Zone. The Axial Zone is characterized by an existence of large ultramafic bodies (Kop and Erzincan ultramafic massifs) and also middle to late Cretaceous ophiolitic olistostromal mélange (Eyuboglu et al., 2007; Eyuboglu et al., 2015b). These zones are separated from each other with NW, NE and EW-trending regional fault zones, which are the main tectonic structures that control the opening and closing of the basins and the emplacement of magmatic bodies and related mineralizations in the region (Eyuboglu et al., 2006, 2015a, Fig. 1).

The study area is situated in the Southern Zone of EPOB (Fig. 1). The oldest rock unit is the Kurtoğlu metamorphic complex, consisting mainly of mica schists, gneisses and metagranitic dikes cutting them. The minimum age of the metamorphic event in this unit is the late Carboniferous at approximately 320 Ma (Topuz et al., 2007). The metamorphic lithologies are cut by the late Carboniferous non-metamorphic Gümüşhane and Köse granitoids, which include many rock types such as granite, granodiorite, quartz diorite, dacite and rhyolite (Topuz et al., 2010; Dokuz, 2011). These basement units are unconformably covered by the early to middle Jurassic Şenköy Formation, which hosts the studied mineralizations. This rift-related formation starts with coarse-grained clastic sedimentary rocks, grades upward with red pelagic limestones of Rosso-Ammonitico facies, continues with a volcano-sedimentary sequence including mainly clastic sedimentary rocks and basaltic–andesitic volcanic and associated pyroclastic rocks and is overlain by late Jurassic to early Cretaceous carbonate rocks (Berdiga Formation) deposited during long-lived thermal subsidence in the entire belt (Eyuboglu et al., 2006). In a recent study, Eyuboglu et al. (2015b) indicated that the basement units of the Şenköy Formation are cut by Aalenian–Bajocian granitic to quartz dioritic intrusions. The late Cretaceous time is represented by a thick turbiditic sequence with interlayered felsic tuffs (Tokel's, 1972 Kermutdere Formation). Zircon U–Pb age determinations from the felsic tuffs indicate that the sequence was deposited on the carbonate platform in Campanian (Eyuboglu, 2015). These pre-Cenozoic lithological units exposed in the Gumushane area are cut by early Eocene adakitic porphyries (Karslı et al., 2010; Eyuboglu et al., 2011a, 2013b) and are uncomfortably covered by the middle Eocene Alibaba Formation including mainly basaltic–andesitic volcanic rocks and their pyroclastic equivalents. All rock units are cut by basaltic dikes of unknown age.

In the Altınpınar mineral field, the late Carboniferous Gümüşhane Granitoid, early to middle Jurassic Şenköy Formation and Eocene Alibaba Formation are the main lithological units (Fig. 3). The Gümüşhane Granitoid is one of the two large plutons exposed in the Southern Zone of EPOB and consists mainly of granite, granodiorite and quartz diorite. However, in the study area, it is represented only

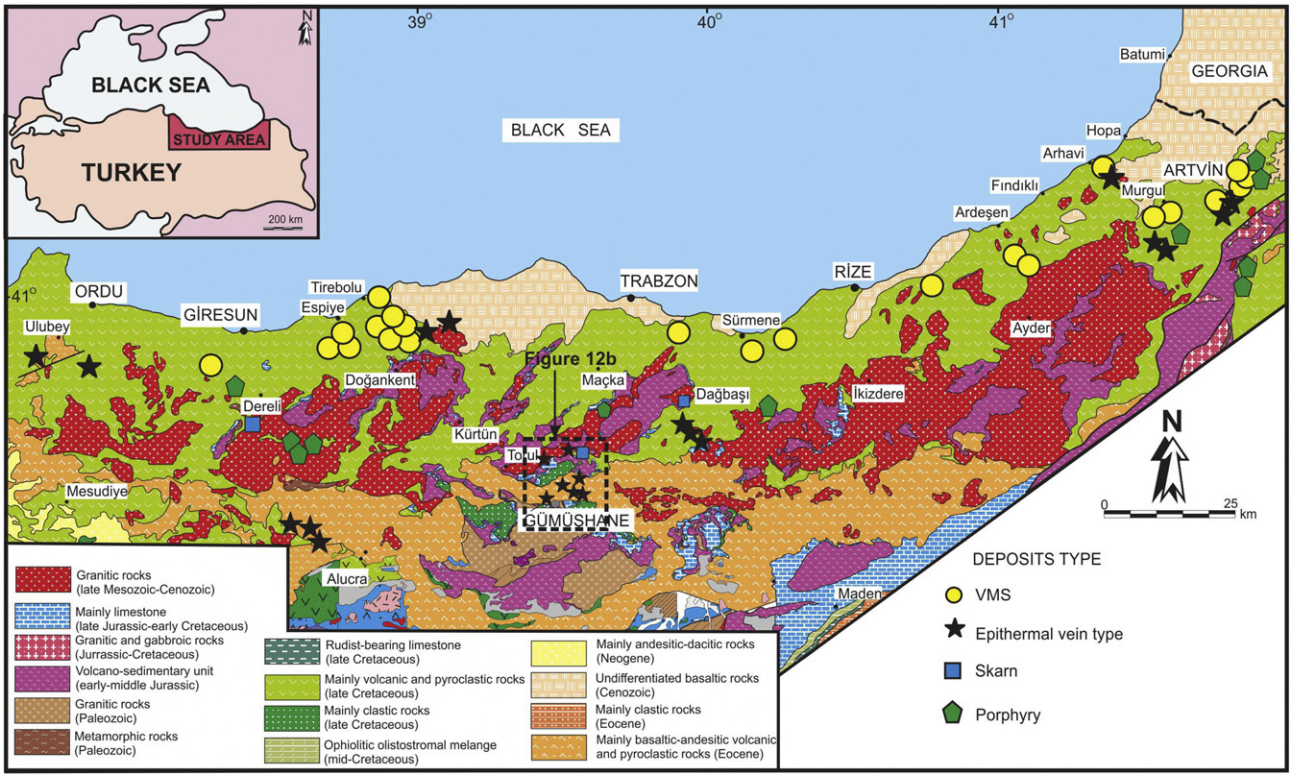

Fig. 2. The geological map, showing the distribution of the main ore deposits in the Eastern Pontides Orogenic Belt. After Eyuboglu et al. (2014).

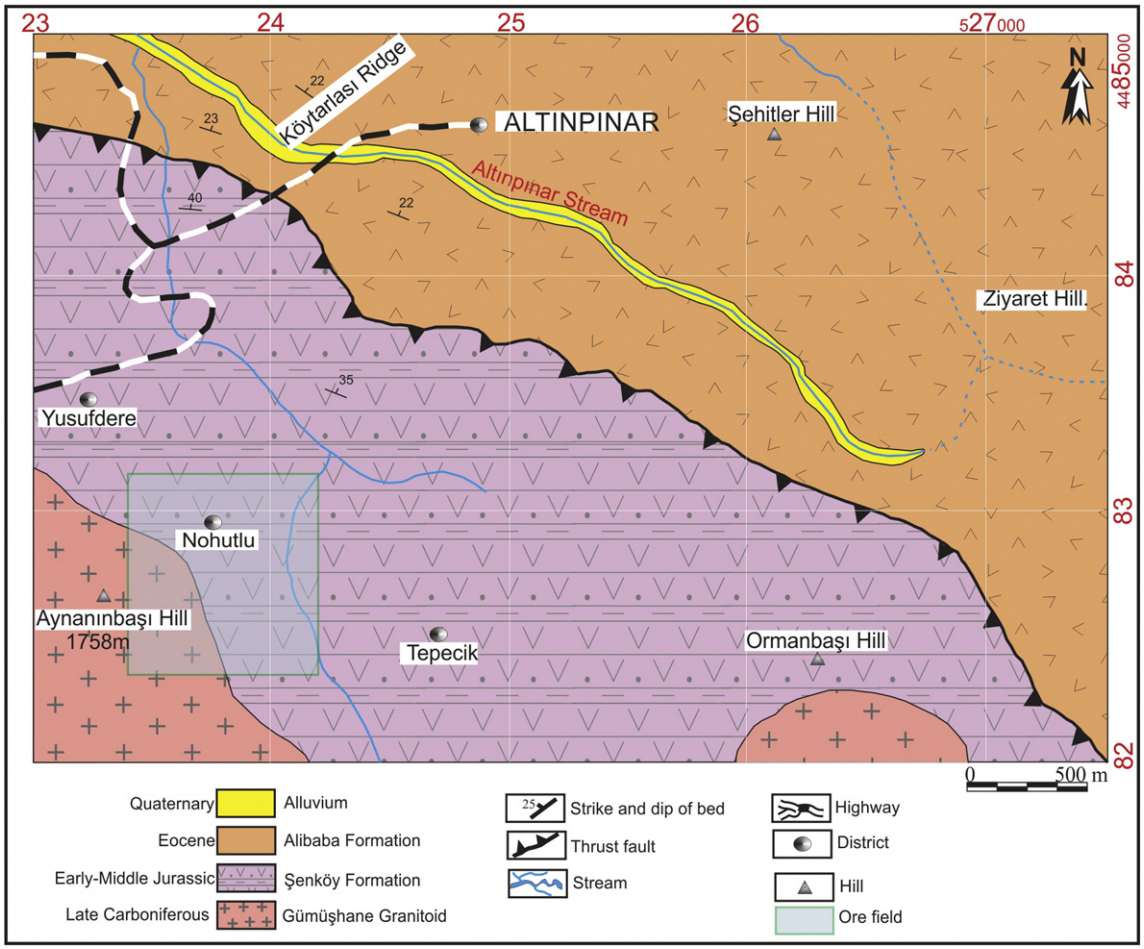

Fig. 3. Geological map of the Altınpınar mineralization field.
After Güner and Yazıcı (2011).

by granite that is well exposed in the southwestern corner of the map area (Fig. 3) and can be easily distinguished from surrounding rocks by its pinkish color owing to high abundances of orthoclase in the rock. It has well-developed fractures that are generally filled by secondary calcite and quartz. The zircon U–Pb age determinations indicated that the Gümüşhane Granitoid is Carboniferous in age (Topuz et al., 2010). The Gümüşhane Granitoid is unconformably covered by an early to middle Jurassic volcano-sedimentary sequence that occurred between the Sinemurian and Callovian stages (Eyuboglu et al., 2015a, 2015b). In the study area, the sequence is represented by basalts and associated pyroclastic rocks that host the mineral systems. The youngest unit exposed in the study area is the Eocene Alibaba Formation, which consists predominantly of basaltic–andesitic volcanic rocks and their pyroclastic equivalents and has a tectonic contact with the early to middle Jurassic Şenköy Formation (Fig. 3).

3. Field characteristics and alteration

The studied Pb–Zn ± Au mineralizations are related to silica veins ranging from a few millimeters to a maximum of 40 cm in thickness and are localized within fracture zones. The main ore occurs in a fracture zone, trending N70°W and dipping 40°SW, extending along the contact between the Gümüşhane Granitoid and Şenköy Formation. Siliceous, sulfidic, hematitic, argillic, chloritic and carbonate alteration are most common around the main mineralization zone (Fig. 4). Chloritic alteration is widespread in the most outer sections of the fracture zone, including the main ore zone, and is easily distinguished from the other alteration types with its green and greenish gray color (Figs. 5b and c), as well as with a brownish green color when in contact with hematitic alteration (Fig. 5a and d). The stockwork of secondary calcite (Fig. 5c), which cut each other, is observed in the fractures with a width of a few millimeters that developed in the intense areas of chloritic alteration. Hematite and limonite are well exposed along the contact between the Gümüşhane Granitoid and Şenköy Formation and also locally in the mineralization site (Fig. 5a). Small-scale and local sulfidation type alteration (Fig. 5d) is observed in the zones near the ore, depending on the disseminated pyrite that develops on quartz veins (Fig. 5e and f), which emerges because of intense silicification in the ore-bearing fracture zones of granitic rocks.

4. Analytical methods

The chemical compositions of pyrite, chalcopyrite, sphalerite, galena and tennantite were measured on a Cameca SX-100 electron probe micro-analyzer (EPMA) at the New Mexico Institute of Mining and Technology, Socorro, NM, USA, using an accelerating voltage of 15 kV and a beam current of 20 nA.

Fluid inclusion analyses were performed at the Mineral Research & Exploration General Directorate (MTA, Ankara). The heating and cooling stages of Linkam MDSG 600 (motorized), which is a fully automatic and programmable system, were used for fluid inclusion studies. The stage was mounted to the Leica DM 2500 M microscope. Lenses with magnifications of 20× and 50× were used for examinations. The Linksys32 software application was used because of its programmability. The temperature intervals of the Linkam stage varied between −196 °C and 600 °C. Heating and cooling rates increased

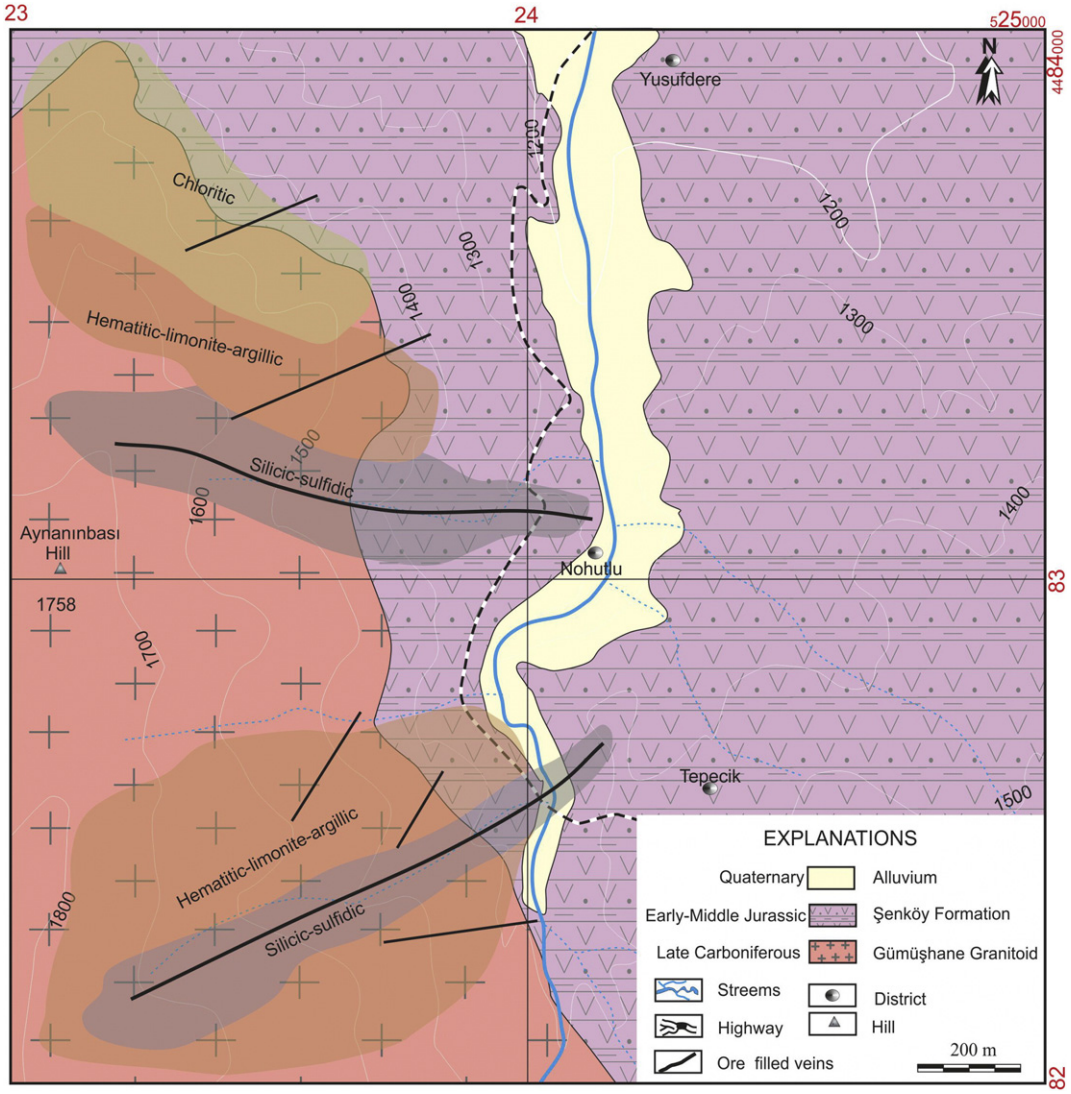

Fig. 4. Alteration map of the Altınpınar mineralization field.

from 0.1 °C/min to 150 °C/min. In the cooling procedures, liquid nitrogen (N_2) was used.

Hydrogen and oxygen isotope analyses were performed on sericite and quartz, respectively, at ACTLAB (Canada). They are reacted with BrF5 at ~650 °C in nickel bombs following the procedures described by Clayton and Mayeda (1963). The fluorination reaction converts O in the mineral(s) to O gas, which is subsequently converted to CO_2 gas using a hot C rod. All reaction steps are quantitative. Isotopic analyses are performed on a Finnigan MAT Delta, dual inlet and isotope ratio mass spectrometer. The data are reported in the standard delta notation as per mil deviations from V-SMOW. External reproducibility is ±0.19‰ (1σ) based on repeated analyses of our internal white crystal standard (WCS). Our value for NBS 28 is 9.61 ± 0.10‰ (1σ). Samples weighing 0.02 to 1.0 g are wrapped in molybdenum foil and placed in a platinum crucible, which is then suspended inside a quartz extraction vessel. The vessel and its contents are outgassed in a vacuum at 120 °C for 4 h to remove surface-adsorbed water. The sample is then inductively heated at 1400 °C for up to 20 min, and the gases are collected in a trap held at −196 °C. Nearly all of the hydrogen is released in the form of water, but miniscule quantities of hydrocarbons or molecular hydrogen released or produced during this treatment are oxidized over CuO at 550 °C to form H_2O and CO, which are also collected in the trap. The accumulated water representing the total amount of hydrogen in the samples is separated from the other gases by differential freezing techniques. The water is reacted with uranium at 900 °C to produce H_2 and collected on charcoal at −196 °C. The volume of the H_2 is measured manometrically. Analyses of the water contents are reproducible to ±0.2 wt.%. Isotopic analyses, conducted by conventional isotope ratio mass spectrometry, are reported in the familiar notation per mil relative to the V-SMOW standard. Duplicate analyses are made of some of these samples, and the δD values agree to better than ±3. Using the procedure described above, we measured a δD value of −65 for the NSB-30 biotite.

For sulfur isotopes, pyrite and galena minerals were analyzed at ACTLAB (Canada). Pure $BaSO_4$ and pure sulfide samples are combusted to SO_2 gas under ~10^{-3} Torr of vacuum. The SO_2 is inlet directly from the vacuum line to the ion source of a VG 602 Isotope Ratio Mass Spectrometer (Ueda and Krouse, 1986). Quantitative combustion to SO_2 is achieved by mixing 5 mg of sample with 100 mg of a V_2O_5 and SiO_2 mixture (1:1). The reaction is carried out at 950 °C for 7 min in a quartz glass reaction tube. Pure copper turnings are used as a catalyst to ensure conversion of SO_3 to SO_2. Internal Lab Standards ($SeaWater_{BaSO4}$ and $Fisher_{BaSO4}$ are run at the beginning and end of each set of samples (typically 25) and are used to normalize the data as well as correct for any instrument drift. All results are reported in the per mil notation relative to the international CDT standard. The precision and reproducibility using this technique are typically better than 0.2‰ (n = 10 internal lab standards).

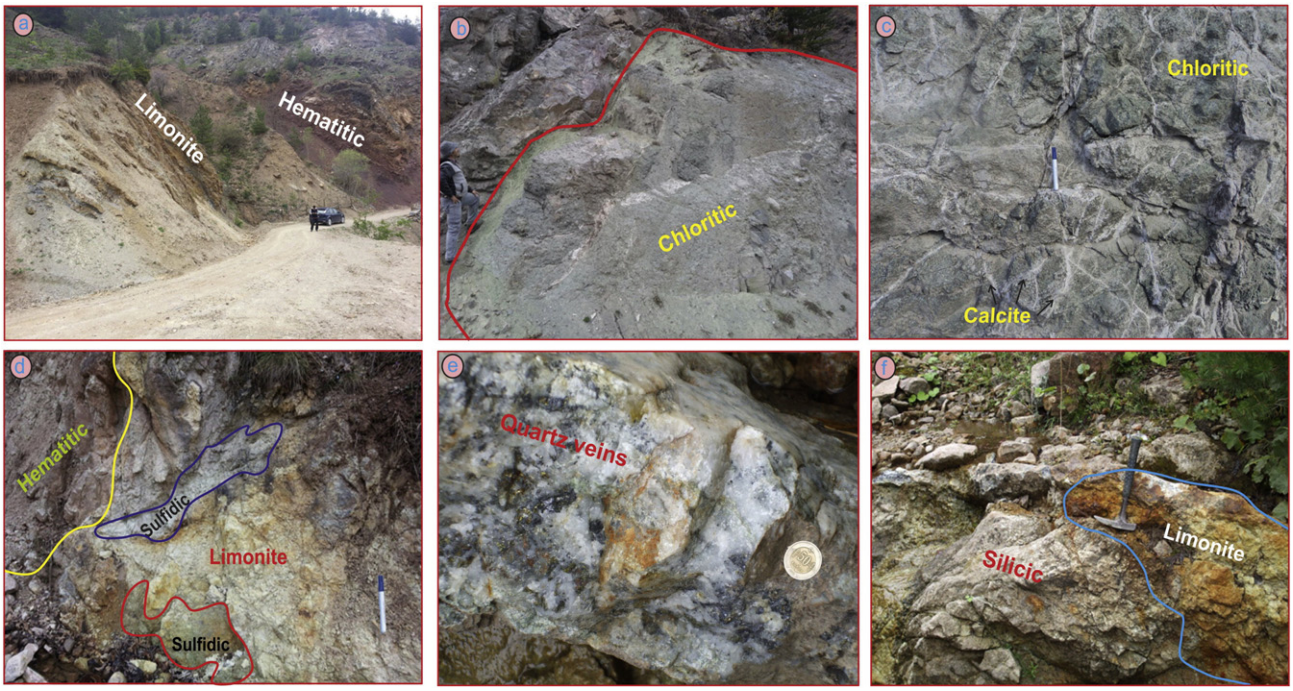

Fig. 5. Field photos showing the relations between mineralization and host rocks and also alterations in the mineralization field.

5. Results

5.1. Ore petrography and mineral chemistry

Microscopic examinations of ore-bearing samples collected from veins in the Altınpınar mineralization field showed that galena, sphalerite, pyrite, chalcopyrite and tennantite are the main ore minerals, whereas quartz is a gangue mineral that is euhedral and presents a jagged and cavity structure, suggesting an existence of epithermal system in their origin. Pyrite, which is the most common observed mineral after galena and sphalerite, presents cataclastic texture and is mostly found in the quartz gangue (Fig. 6b and c); pyrite is sometimes observed anhedrally as residual inclusions from replacement within chalcopyrite. Microprobe analysis showed that pyrites do not contain significant amounts of Cu and Zn (Table 1). Chalcopyrite, which is found in the quartz gangue and mostly precipitated simultaneously with galena (Fig. 6f), is anhedral and present exsolution texture within sphalerite. Chalcopyrite includes low amounts of Zn (0.01–0.33 wt.%). Galena, which is easily recognized by their grayish white reflection and present triangular pits in their euhedral minerals, is the most abundant ore

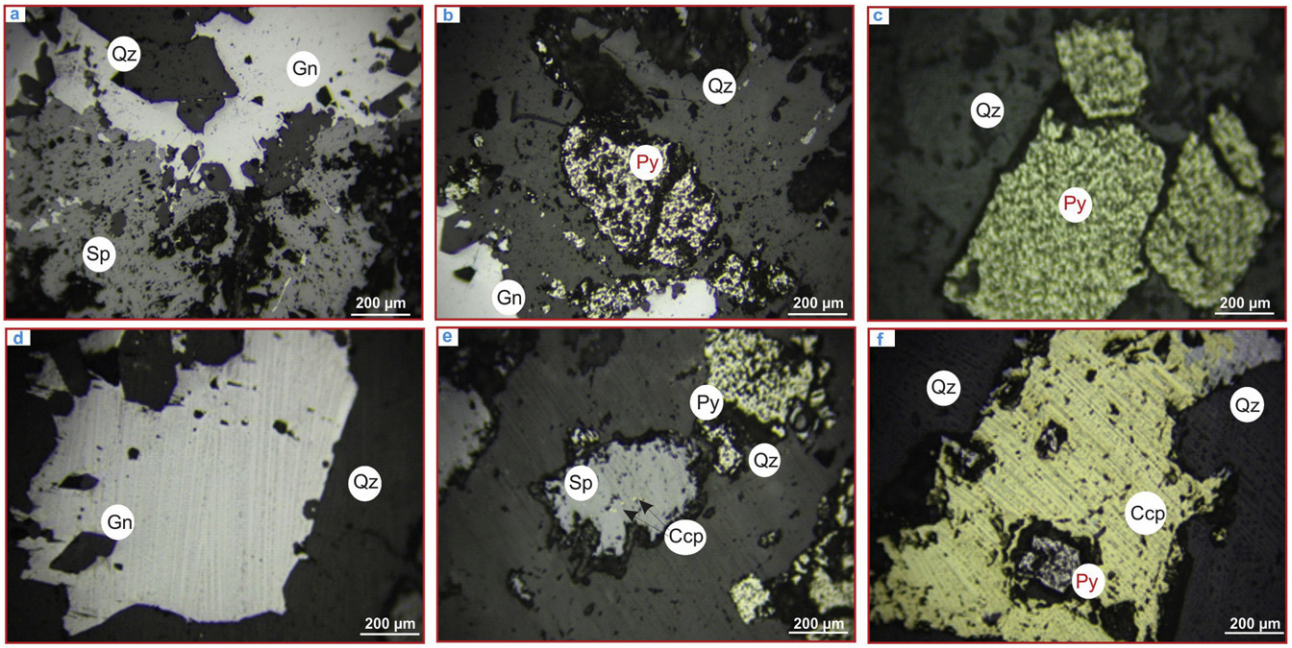

Fig. 6. Photomicrographs taken under reflected light images showing the textural relations among the ore minerals in the studied mineralization. (a) Replacement of galena by sphalerite and euhedral quartz with jagged structure, (b) quartz gangue and cataclastic Pyrite, (c) cataclastic texture in pyrite, (d) galena and euhedral quartz, (e) chalcopyrite exsolutions in sphalerite, (f) pyrite inclusions in chalcopyrite (Qz: quartz, Gn: galena, Sp: sphalerite, Py: pyrite, Ccp: chalcopyrite, Scale bar = 200 µm).

Table 1
Statistical data of microchemical analysis of ore minerals.

			S wt.%	Fe wt.%	Cu wt.%	Zn wt.%	Mn wt.%	Cd wt.%	Sb wt.%	As wt.%	Ag wt.%	Au wt.%	Pb wt.%	Zn/Cd
Pyrite	n = 19	Min.	51.55	45.54	0.00	0.01								
		Max.	54.85	47.89	0.22	0.50								
		Mean	53.36	46.38	0.08	0.9								
Chalcopyrite	n = 9	Min.	34.08	29.63	33.48	0.01								
		Max.	34.79	30.57	33.97	0.33								
		Mean	34.39	30.18	33.71	0.05								
Sphalerite	n = 20	Min.	32.34	0.01	0.01	61.75	0.01	0.44						50.65
		Max.	33.51	1.42	1.24	64.42	0.15	1.48						144.64
		Mean	32.81	0.59	0.23	63.4	0.04	0.75						94.77
Tennantite	n = 6	Min.	26.67	0.59	31.25	8.81			0.01	19.35	0.03	0.01	0.05	
		Max.	28.22	1.53	37.96	12.11			0.14	21.33	0.05	0.03	0.19	
		Mean	27.68	0.87	35.16	10.19			0.03	20.46	0.04	0.02	0.10	

mineral in sphalerite (Fig. 6a and d). Ore microscopy examinations showed that galena coexists mostly with the sphalerite. Microchemical analysis demonstrated that galena does not contain any trace elements and is crystallized similarly to the stoichiometric composition. Sphalerite presents darker gray colors than galena, exhibits a replacement relationship with galena and forms an exsolution texture, which signifies its concurrent formation with chalcopyrite mineral (Fig. 6a and e). Microprobe analysis indicates that Fe, among trace elements, features the elemental characteristic that mostly suits Zn ($r = 0.50$), which is the main component of sphalerite (Fig. 7a). This highly negative correlation between Fe and Zn shows that Fe substitutes for Zn as a function of temperature, and these elements can be used as sphalerite geobarometers (Scott and Barnes, 1971; Browne and Lowering, 1973). In the ore microscopy studies conducted using polished sections prepared from the samples of the Altınpınar mineralization site, the Fahlerz group minerals, which are determined as the uncommon minerals among all ore minerals, and generally amorphous grains are observed as exsolutions within galena minerals. Considering microchemical data (Fig. 7b and Table 1), Fahlerz minerals in the studied mineralization are tennantite in composition with high contents of As (19.35–21.33 wt.%) and low contents of Sb (0.01–0.14 wt.%). Fahlerz also includes 0.01–0.03 wt.% Au and 0.05–0.19 wt.% Pb (Table 1).

5.2. Fluid inclusions

Microthermometric measurements were taken on the quartz mineral in single-phase (liquid), which constitutes a major part of primary inclusions, and two-phase (liquid + gas) inclusions. Primary single-phase (liquid) and two-phase (liquid + gas) inclusions occur as irregular, circular, ellipsoid, lenticular, triangular, square and/or rectangular shapes in quartz (Fig. 8a–d). The sizes of single-phase inclusions vary between <1 and 20 μm. The sizes of the two-phase (liquid + gas) inclusions vary between <1 and 8 μm, and some inclusions even reach 15–16 μm. The ratio of the liquid phase to the gaseous phase is high in the primary two-stage inclusions. Fluid inclusion examinations showed that some primary two-phase inclusions also contain daughter minerals. However, the composition of these daughter minerals could not be identified. In the Altınpınar mineralization, the ice melting temperatures measured in the quartzes are between −4.6 °C and −1.4 °C (−2.9 °C on average), and the salinity of the fluids in the quartz samples calculated by Bodnar (1993) is 4.7 wt% NaCl eqv. on average. When the frequency distribution graphics of the homogenization temperatures (T_h) prepared per T_h values are reviewed in Fig. 9, T_h values vary between 170 °C and 380 °C and are condensed at 250–300 °C.

5.3. Hydrogen and oxygen isotopic systematics

In the Altınpınar mineralization, H isotope analyses were conducted on three sericite minerals, whereas O isotope analyses were conducted on three quartz minerals. The results are given in Table 2. The oxygen and hydrogen isotope analyses results vary between 8.5‰ to 10.2‰ and −91‰ to −73‰, respectively. This variation shows that the oxygen and hydrogen isotope compositions are similar to those of both surface and magmatic waters (Hoefs, 1987). The $\delta^{18}O$ compositions of fluids were balanced with quartz and calculated using $\Delta_{quartz\text{-}fluid} = \delta^{18}O_{quartz} - \delta^{18}O_{fluid} = 3.38 \times (10^6/T^2) - 2.90$ (O'Neil and Taylor, 1969) with the homogenization temperature value (277 °C) measured from the fluid inclusions in quartzes. The $\delta^{18}O$ composition of the fluids balanced with quartz varies between 0.31 and 2.01.

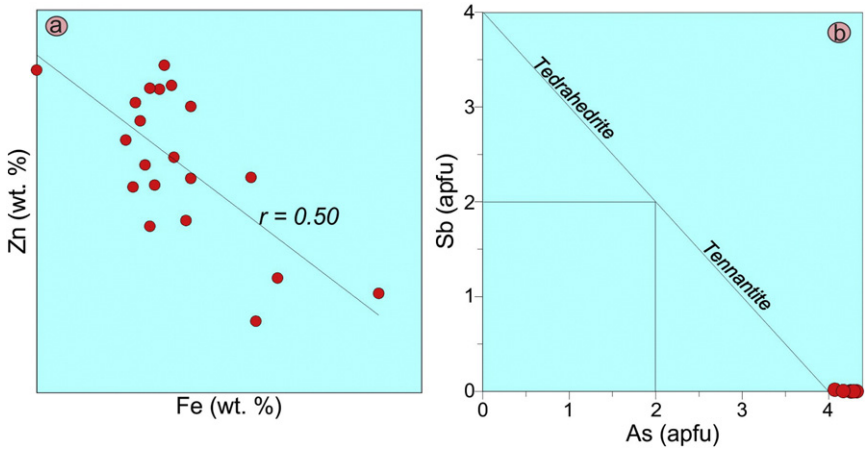

Fig. 7. (a) Fe versus Zn variations in sphalerite, (b) compositional variations of fahlores on As versus Sb plots.

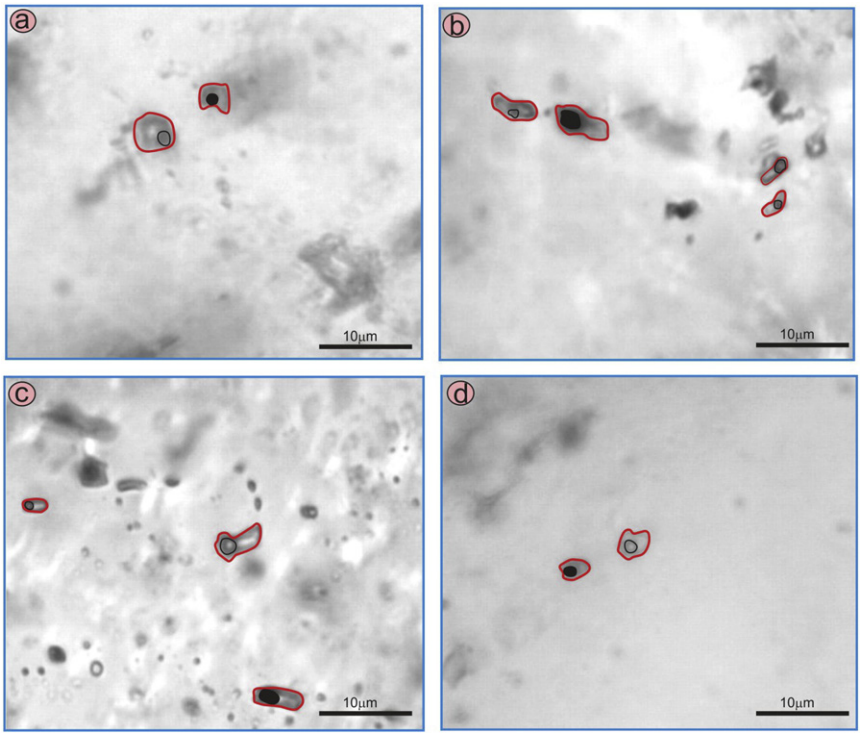

Fig. 8. Photomicrographs showing of the fluid inclusions in quartz. (a, d) Irregular shaped liquid + gas inclusions, (c, d) ellipsoid shaped liquid + gas inclusions.

5.4. Sulfur isotopic compositions

Sulfur isotope analyses ($\delta^{34}S$) were performed on pyrite and galena minerals, and the results obtained, which range from −8.3‰ to −2.3‰, are presented in Table 3. The temperatures of ore formation calculated using a sulfur geothermometer vary between 264 and 370 ± 20 °C with an average temperature of 317 ± 20 °C, which is consistent with the homogenization temperatures obtained from fluid inclusions (Fig. 9).

Compared to the isotope data of various geological environment, rock and ore types reported in previous studies (Ohmoto and Rye, 1979; Field and Fifarek, 1985; Hoefs, 1987), it is clear that our results are consistent with the $\delta^{34}S$ values of granitic rocks and base metal vein-type deposits, which indicate magmatic sulfur (Cooke and Simmons, 2000; Hedenquist et al., 1994). Sulfur was present mainly as HS^- and S^{2-}, and the $\delta^{34}S$ values of deposited pyrite and galena can therefore indicate $\delta^{34}S$ of S in the ore-forming fluid (Ohmoto, 1972; Ohmoto and Rye, 1979). Data in this study for $\delta^{34}S$ from the hydrothermal fluid systems in the deposit reveal a very narrow compositional range, indicating that the sulfur was derived from the mantle source (Hoefs, 1987; Gemmell and Large, 1992).

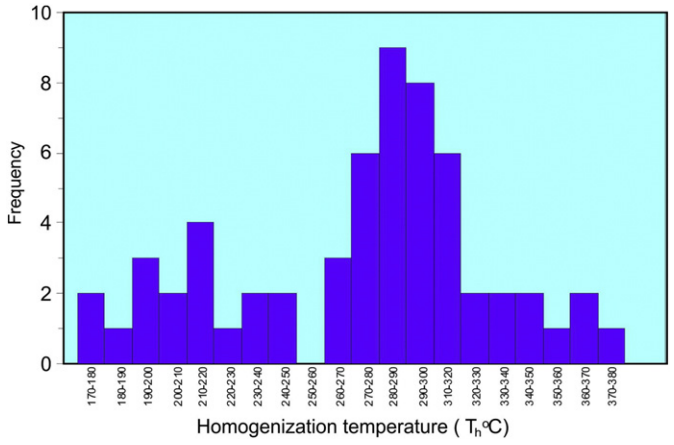

Fig. 9. Frequency chart showing the distribution of homogenization temperatures of fluid inclusion in quartz.

6. Discussion

6.1. Ore-forming material sources

The Zn/Cd ratio of sphalerite is important for determining the mineralization type. Song (1984) suggested that the Zn/Cd ratio is between 104 and 214 in hydrothermal deposits (including volcano-hydrothermal deposits), 252 and 330 in metamorphosed sedimentary deposits and carbonate-hosted strata-bound and stratiform deposits and 417 and 531 in volcano-sedimentary type deposits. Similarly, Gottesmann and Kampe (2007) suggested that the Zn/Cd ratio is >477 in the mineralizations related to basaltic magmas, between 328 and 427 in the mineralizations related to andesitic magmas, <300 in the mineralizations related to rhyolitic magmas and below 250 in the hydrothermal deposits related to granitic magmas. Microchemical studies reveal that the Zn/Cd ratio of sphalerite minerals varies between 50.65 and 144.64 (Table 1), supporting that the Altınpınar mineralization is a hydrothermal deposit related to granitic magmatism.

The coexistence of the liquid- and gas-enriched inclusions in quartz suggests an open system during their evolution, except for fluid inclusions that form as a result of necking down and ranges on the same line (Roedder, 1984; Shepherd et al., 1985). The coexistence of both liquid and gas-rich inclusions in quartzes and their random distribution clearly indicate that Altınpınar mineralization occurred in the open system, and the measured inclusions are not a result of necking down.

The sources of hydrothermal solutions in the low-sulfidation epithermal systems are dominantly meteoric and rarely magmatic (Giggenbach, 1992; Hedenquist and Lowenstern, 1994; Matsuhisa and Aoki, 1994). Only a limited number of studies have been conducted on the fluid inclusions in quartzes and O-H isotopes in alteration minerals observed in the epithermal vein-type mineralization fields exposed in

Table 2
Stable isotope data from Altınpınar mineralizations.

Location	Sample	Mineral	$\delta^{18}O$ ‰	Sample	Mineral	δD ‰
	H9	Quartz	9.8	A3	Sericite	−91
	H11	Quartz	10.2	A7	Sericite	−79
Altınpınar Pb-Zn ± Au (this study)	H13	Quartz	8.5	A15	Sericite	−73
	L1	Quartz	15	C2	Sericite	−91
	L2	Quartz	14.5	C11	Sericite	−87
Arzular Au ± Ag (Akaryalı and Tüysüz, 2013)	L3	Quartz	16.7	D12	Sericite	−93
	GR	Quartz	11.3	GR	Quartz	−63
	B1280K	Quartz	10.3	B1280K	Quartz	−66
	D1265K	Quartz	10.2	D1265K	Quartz	−56
	G5	Quartz	10.5	G5	Quartz	−71
	O1	Quartz	11	O1	Quartz	−64
	YD1-2	Quartz	11.5	YD1-2	Quartz	−64
	O3	Quartz	11.2	O3	Quartz	−84
	O6	Quartz	11.4	O6	Quartz	−77
	YD2-3	Quartz	9.8	YD2-3	Quartz	−79
	B1340G	Quartz	10.2	B1340G	Quartz	−78
	KMK-10	Illite-kaolin	8.1	KMK-10	Illite-kaolin	−96
	KMK15	Illite	9.5	KMK15	Illite	−60
	KZM46/11	Illite	8.3	KZM46/11	Illite	−72
	KMK100	Illite	12.4	KMK100	Illite	−81
	KMK70	Smectite-kaolin	10.8	KMK70	Smectite-kaolin	−67
Mastra Au–Ag (Aslan, 2011)	KMK23	Smectite-kaolin	12.3	KMK23	Smectite-kaolin	−63
	MA1	Quartz	10.6	MA1	Fluid in quartz inclusion	−97
	MA2	Quartz	10.5	MA2	Fluid in quartz inclusion	−94
	MA3	Quartz	10.9	MA3	Fluid in quartz inclusion	−92
	MA4	Quartz	9.9	MA4	Fluid in quartz inclusion	−88
	MA5	Quartz	9.8	MA5	Fluid in quartz inclusion	−92
	MA6	Quartz	13.2	MA6	Fluid in quartz inclusion	−93
	MA7	Quartz	11.3	MA7	Fluid in quartz inclusion	−84
	MA8	Quartz	10.9	MA8	Fluid in quartz inclusion	−90
	MA9	Quartz	11.0	MA9	Fluid in quartz inclusion	−79
	MA10	Quartz	17.8	MA10	Fluid in quartz inclusion	−85
	MA11	Quartz	11.5	MA11	Fluid in quartz inclusion	−84
Mastra Au–Ag (Tayyar, 2005)	MA12	Quartz	11.0	MA12	Fluid in quartz inclusion	−79

the Southern Zone of EPOB (e.g., Lermi, 2003; Tayyar, 2005; Aslan, 2011; Akaryalı and Tüysüz, 2013; Figs. 10 and 11). Fluid inclusion studies indicate that there is a close relationship between homogenization temperature and salinity (e.g., Shepherd et al., 1985; Wilkinson, 2001), and the type of ore deposit can be determined using these values (Roedder, 1984). In the Altınpınar mineralization, the homogenization temperatures measured from fluid inclusions vary between 170 °C and 380 °C, especially between 250 °C and 300 °C, and the wt.% NaCl eqv. Salinity of ore-forming fluids is between 2.4 and 7.3 (4.7 on average). These results are consistent with the results presented in the previous studies and indicate dilution by surface-derived waters (Fig. 10a). On the salinity versus homogenization temperature discrimination diagram (Roedder, 1984), they fall into field of epithermal vein-type deposits (Fig. 10b). The values of oxygen and hydrogen isotopes obtained from quartz and sericite vary between 8.5‰ and 10.2‰ and −91‰ and −73‰, respectively, indicating that hydrothermal solutions that produced Altınpınar mineralization were derived from a mixture of magmatic and meteoric waters (Fig. 11).

Table 3
Sulfur isotope data from Altınpınar mineralizations [equilibrium temperature of pyrite–galena (T1), sphalerite–galena (T2) and pyrite–sphalerite (T3) mineral pairs].

Location	Sample no	Pyrite ‰	Chalcopyrite ‰	Sphalerite ‰	Galena ‰	T1 °C (py–gn)	T2 °C (sph–gn)	T3 °C (py–sph)
	H9	−2.3			−4.7	370 ± 20		
	H11	−2.8			−6.3	264 ± 20		
Altınpınar Pb–Zn ± Au (this study)	H13	−8.3			−2.9			
	TG2-61	6.7		4.4	2.5		347 ± 25	
	TG2-82	3.9		5.3	3.3		331 ± 25	
	TG1-22	5.2		5.2	3.1		313 ± 21	
Midi Pb-Zn (Lermi, 2003)	Hd11b	5.1		2.0	4.3		232 ± 20	
	L1	3		0	−0.7	251 ± 20		
	L2	2.2			−0.6	291 ± 20		
Arzular Au ± Ag (Akaryalı and Tüysüz, 2013)	L3	2.6		−0.5	−1.2	244 ± 20		
	O1			−3.5	−6.2		254 ± 19	
	O2			−3.5	−5.6		313 ± 21	
	O3			−4	−6		328 ± 21	
	O4			−3.6	−5.4		360 ± 22	
	O5	−2.9	−3.6					
	O6	−3.1		−2.3				
	O7	−3.2	−3.3	−1.7	−5.8	353 ± 20	147 ± 15	
	G2	−3		−3.7				384 ± 48
	G5		−3.6		4.6			
Mastra Au–Ag (Aslan, 2011)	G8			−2.7	−4.8		313 ± 21	

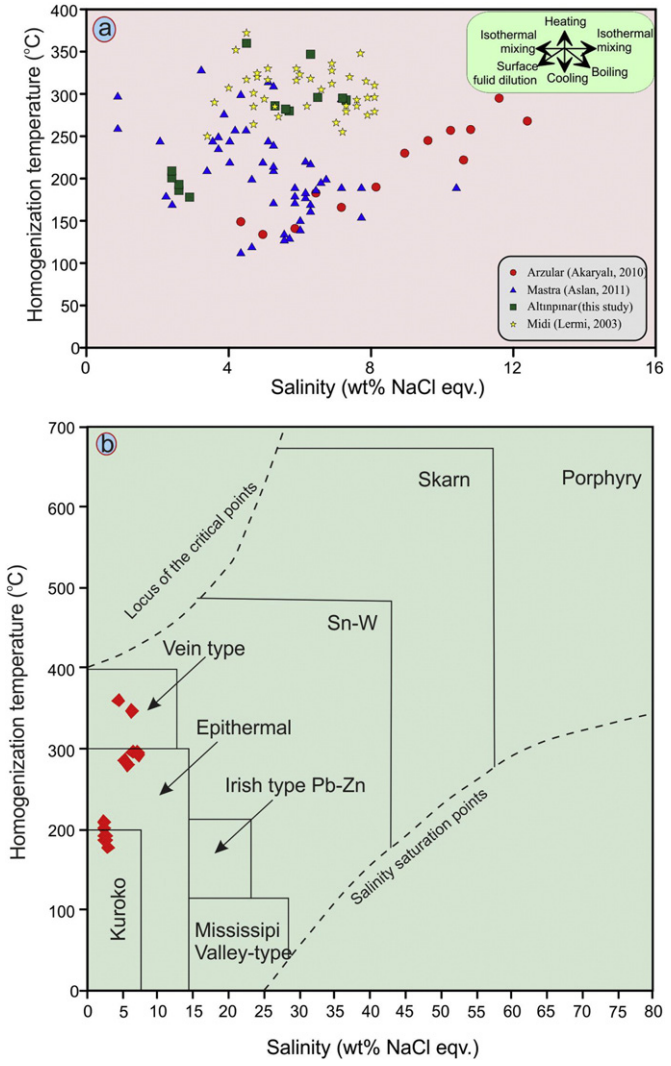

Fig. 10. (a) Schematic diagram showing typical trends in homogenization temperatures-salinity space due to various fluid evolution processes (after Wilkinson, 2001), (b) homogenization temperature and wt.% NaCl eqv. diagram (Roedder, 1984) for fluid inclusions in quartz.

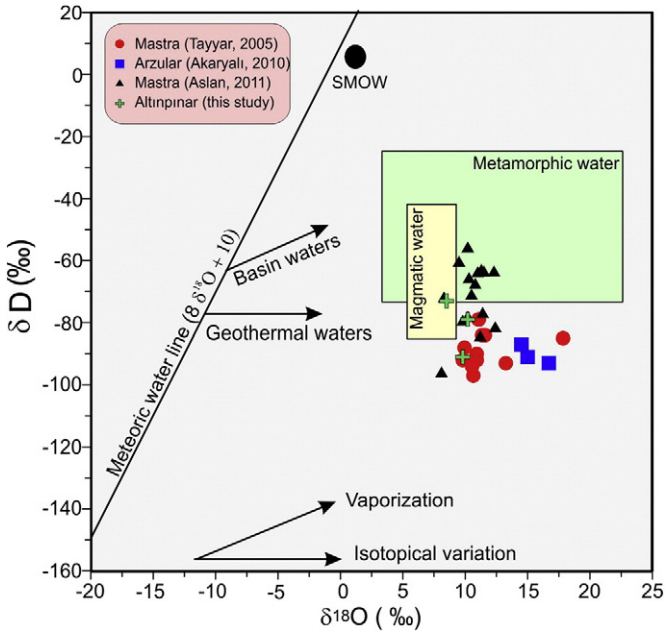

Fig. 11. δD (‰) versus $\delta^{18}O$ (‰) diagram showing the distributions of the hydrogen isotope values in sericite and oxygen isotope values in quartz from the Altınpınar mineralization field (after Taylor, 1974 and Ohmoto, 1986; SMOW: Standard Mean Ocean Water).

6.2. Ore genesis

The epithermal mineralizations can be divided into two main groups of low- and high-sulfidation deposits based on sulfur content (e.g., Hedenquist et al., 1994). The low-sulfidation deposits are characterized by hosting in intermediate volcanic rocks occurring in the fracture zones; the existence of sericite, illite and chlorite as alteration minerals; and the formation temperature changing by 100 and 300 °C (Barton and Skinner, 1979; Henley and Ellis, 1983; Ransome, 1907; Hedenquist et al., 1994; White and Hedenquist, 1990; Heald et al., 1987). The high-sulfidation deposits are different from the low-sulfidation deposits with their host rocks comprising felsic volcanic rocks, alteration minerals including mainly kaolinite and alunite and high formation temperature. The Altınpınar mineralization is hosted by basaltic–andesitic volcanic rocks consisting mainly of plagioclase, pyroxene and amphibole are that extensively altered to sericite and chlorite in the mineralization field. Sulfur isotope studies reveal that the formation temperature for the Altınpınar mineralization is between 264 and 370 °C. Considering all data, it is clear that the studied mineralization carries the traces of low-sulfidation epithermal deposits. The formation depth and pressure of ore deposits can be calculated using homogenization temperatures obtained from fluid inclusion (Roedder and Bodnar, 1980; Roedder, 1984; Shepherd et al., 1985; Knight and Bodnar, 1989). Several numerical models have been developed to represent the PVTX properties of H_2O–NaCl, facilitating interpretation of data from fluid inclusions. In this study, HOKIEFLINCS_H_2O-NACL program (Steele-MacInnis et al., 2012) is used for depth and pressure of Altınpınar mineralizations. HOKIEFLINCS_H_2O-NACL can be used to determine the properties of fluid inclusions that homogenize to the liquid phase. The program is generally valid from −21.2 to 700 °C, the LV curve to 6000 bar and 0 to 70 wt.% NaCl for fluid inclusions that homogenize by vapor bubble disappearance; and from T_h of 100 to 600 °C, the LVH curve to 3000 bar and 28–75 wt.% NaCl for fluid inclusions that homogenize by halite disappearance.

Aslan (2011) concluded that the Mastra gold mineralization, which is one of the most economical mines in the Alpine–Himalayan belt, formed under changing pressures between 690 and 460 bar, indicating that the formation depth is between 2605 and 1737 m. Similarly, Lermi (2003) suggested that Midi Pb–Zn mineralization, which is situated 19 km south of Mastra gold mineralization (Fig. 12b), formed at the depth of 1963 m and under the pressure of 520 bar. According to the HOKIEFLINCS_H_2O-NACL program, the trapping pressure has been calculated to vary between 62 and 181 bar (average 94 bar), indicating that the formation depth is between 630 and 1842 m (average 963 m) in Altınpınar mineralizations. The Altınpınar mineralization has a very similar trapping pressure and formation depth as well as geological and geochemical characteristics to those of Mastra and Midi mineralizations, supporting that a similar magmatic source has played an important role formation in the three mineralizations.

Detailed studies about vein-type mineralizations are limited in the northern part of the EPOB (e.g., Gökçe and Bozkaya, 2003; Bozkaya and Gökçe, 2003; Kudun-Yozgat, 2009; Yaylalı-Abanuz and Tüysüz, 2010; Demir et al., 2015). Bozkaya and Gökçe (2003) indicated that sulfur in the Inler Yaylası (Giresun, NE Turkey) lead zinc mine hosted by extensively altered, Upper Cretaceous volcano-sedimentary rocks had originated from magmatic sources according to the isotope values ranging from −3.9 to 0.4‰. Similarly, Demir et al. (2015) reported that the $\delta^{34}S$ compositions of sulfur isotope varied between 2.14 and −1.47‰, and the oxygen and hydrogen isotope compositions varied between 7.8 and 8.5‰ and −40 and 57‰, respectively in the Kabadüz (Ordu, NE Turkey) ore veins that occur in the Upper Cretaceous andesitic

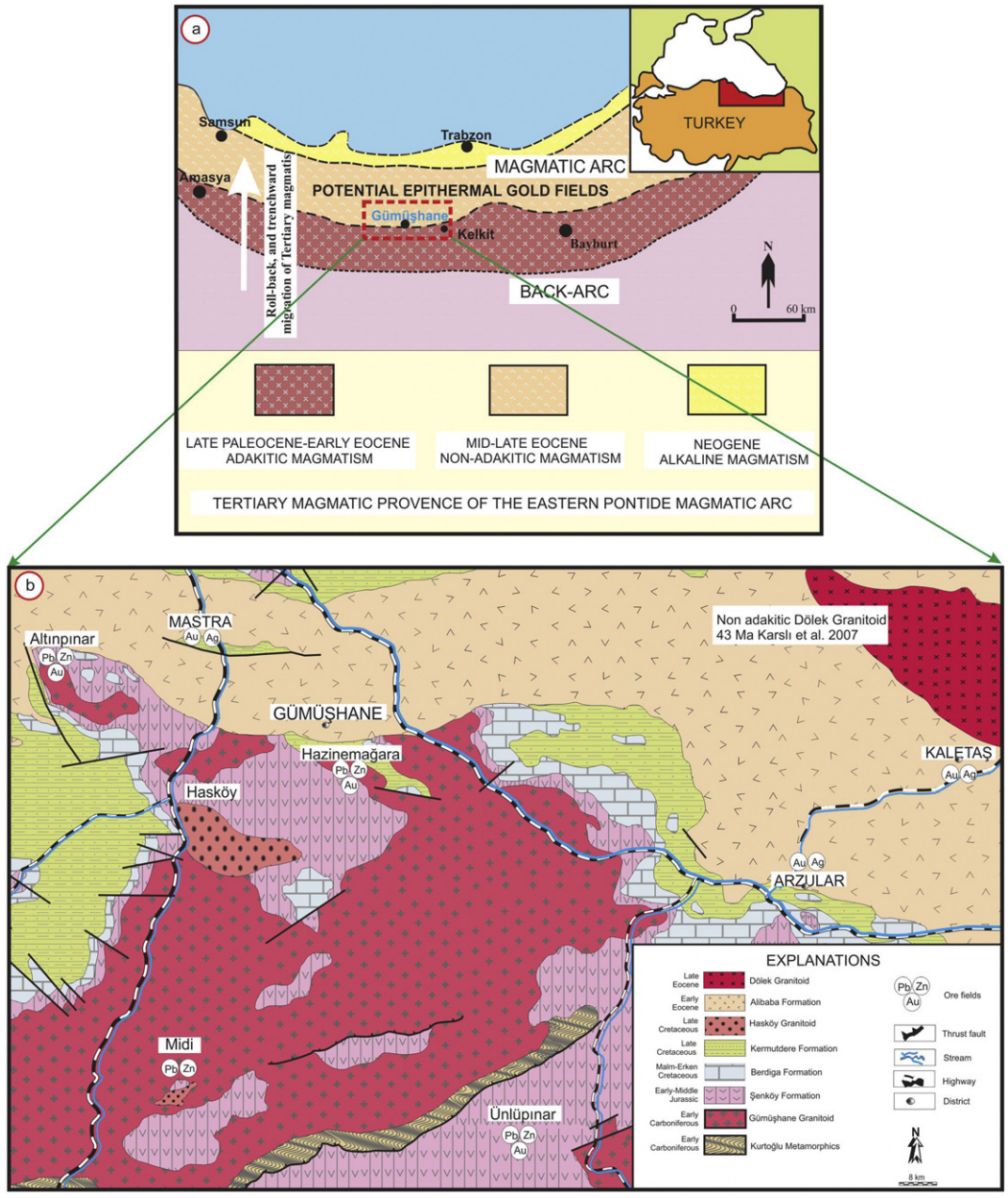

Fig. 12. a) Early Cenozoic magma series and potential epithermal gold fields of the Eastern Pontides Orogenic Belt (Eyuboglu et al., 2011c). b) Generalized geological map of the Gümüşhane area (after from Güven 1993).

rocks. The authors suggested that Kabadüz mineralization is associated with younger granitic intrusions than those in the Upper Cretaceous. Akoluk (Ordu) vein-type mineralization occurs along fault systems in dacitic tuffs of Upper Cretaceous age in the northern part of the EPOB. Yaylalı-Abanuz and Tüysüz (2010) suggested that the presence of framboidal and colloidal ore minerals and textures indicated that Akoluk (Ordu) vein-type mineralization occurred at low temperatures in an epithermal system. To summarize, mineralizations in the northern part of EPOB are associated with the Upper Cretaceous volcanic rocks. Unlike the northern zone, mineralizations in the southern part of EPOB occur in Eocene and Jurassic rocks. However, stable isotope (S, O and H) composition of mineralization in the northern and southern zones are similar, which implies a magmatic source in the formation of mineralizations.

Burnham and Ohmoto (1980) proposed that granitic magmas are responsible for the formation of various mineralizations such as porphyry, skarn and epithermal. The sulfur isotope values obtained from both this and previous studies in the Gümüşhane region located on the Southern Zone of EPOB (Lermi, 2003; Aslan, 2011; Akaryalı and Tüysüz, 2013) vary in range from −8.2‰ to 2‰ (Table 3). This relatively tight clustering of sulfur isotope values can be interpreted to indicate that the fluid redox state was below the SO_2/H_2S boundary, and H_2S was the dominant reduced sulfur species in the fluids. In addition, this range of isotope values can support an origin related to granitic magmas (Ohmoto and Rye, 1979). Considering all geological, geochemical and geochronological data obtained from the granitic bodies exposed in the Gumushane region (Karsli et al., 2007; Kaygusuz et al., 2008; Eyuboglu et al., 2011a, 2011b, 2013a, 2015b), the studied epithermal vein-type mineralizations hosted by early to middle Jurassic volcanic rocks could be produced by middle Jurassic, late Cretaceous or Eocene granitic magmas. However, Mastra and Arzular gold mineralizations occur in basaltic–andesitic lithologies of Eocene Alibaba Formation, supporting that their origin is related to Eocene or later granitic magmas. Eyuboglu et al. (2011a, 2013a) suggested that the Eocene

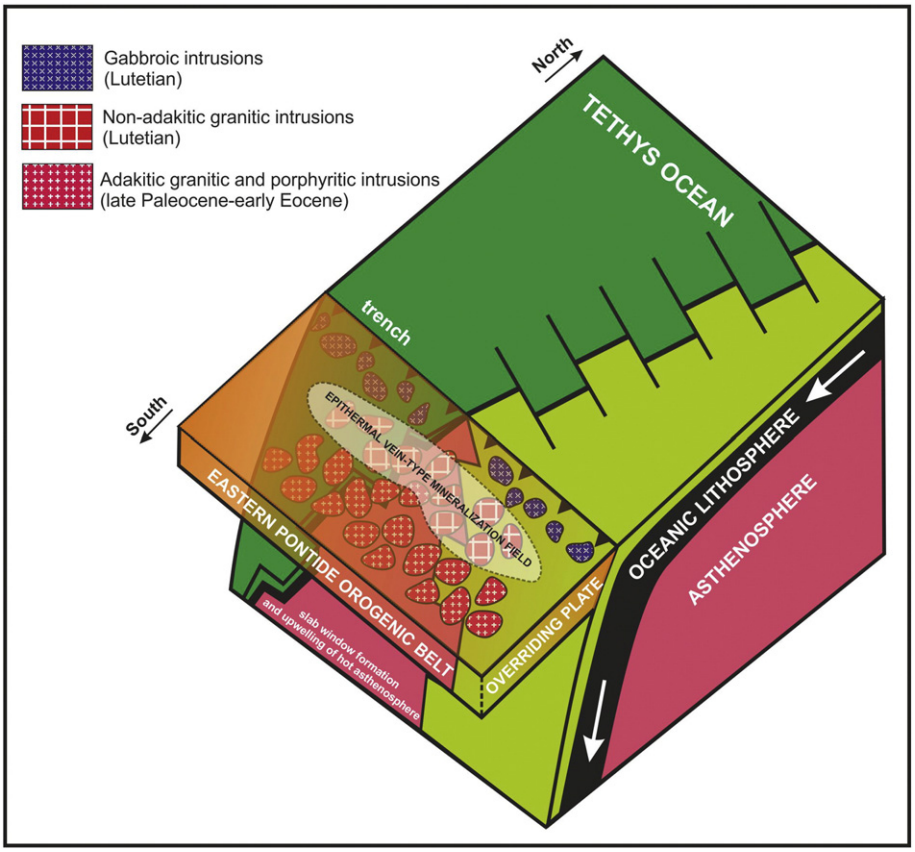

Fig. 13. Cartoon diagram showing the formation of the Lutetian granitic magmas and related epithermal vein-type mineralizations in the Southern Zone of EPOB. Modified from Eyuboglu et al. (2015a).

granitic magmas were generated in a slab window-related setting and occurred at two different cycles in the southern part of eastern Pontides. The first cycle is represented by adakitic intrusions exposed in the south of the Torul–Bayburt–Ispir line. The second cycle of granitic magmatism is represented by non-adakitic intrusions that are well exposed immediately north of the Torul–Bayburt–Ispir line (Fig. 12a). According to Eyuboglu et al. (2011c), the adakitic intrusions exposed in the southern part of EPOB are devoid of ore deposits, which leads us to propose that the Lutetian or later non-adakitic granitic intrusions, which are exposed at the north of the Gumushane–Bayburt–Ispir line, were probably responsible for the epithermal gold mineralization in this belt. All data obtained from this study supports their idea that the epithermal vein-type mineralizations in the Southern Zone of EPOB are related to non-adakitic Lutetian granitic magmas (Fig. 13).

7. Conclusions

The main conclusions of this study focusing on the geology, mineralogy and genesis of the Altınpınar mineralization (Torul–Gümüşhane, NE-Turkey) located in the Southern Zone of the Eastern Pontides Orogenic Belt are summarized below.

- Altınpınar mineralization is well exposed along the contact between Carboniferous Gümüşhane Granitoid and basaltic rocks of the early to middle Jurassic Şenköy Formation and is related to silica veins ranging from a few millimeters to a maximum of 40 cm in thickness.
- The main ore minerals are sphalerite, galena, pyrite, chalcopyrite and tennantite, whereas quartz is mostly found as the gangue mineral. The jagged and cavity structure of the quartz minerals points to an epithermal system.
- Microchemical analyses conducted on sphalerite minerals showed that the Zn/Cd ratios vary between 50.65 and 144.64, indicating that the studied mineralization is related to granitic magmas.
- The homogenization temperatures measured from the fluid inclusions vary between 170 °C and 380 °C, the condensation varies from 250 to 300 °C (277 °C on average), and the wt.% NaCl eqv. salinity of ore-forming fluids varies between 2.4 and 7.3 (4.7 on average). These findings indicate that the mineralization developed in the epithermal system.
- The values obtained in sulfur isotope analysis conducted on pyrite and galena minerals are between −8.3‰ and −2.3‰. This variation shows that sulfur, which enables mineral formation, originates from magmatic genesis. The average formation temperature of the ore calculated using a sulfur isotope thermometer is 317 °C.
- Oxygen isotope values range between 8.5‰ and 10.2‰, and hydrogen values vary between −91‰ and −73‰. Accordingly, the fluids that formed the mineralization are magmatic and mixed with surface waters.
- Considering all geological, geochemical and isotopic data, it is clear that the Altınpınar mineralization is an epithermal vein-type mineralization and is related to non-adakitic granitic magmas produced in the Southern Zone of the Eastern Pontides Orogenic Belt in Lutetian.

Acknowledgments

This study was funded by The Scientific and Technological Research Council of Turkey (TÜBİTAK Grant No: 113Y381). The author is grateful to handling editor M. Santosh and to anonymous reviewers for their critical and constructive comments to improve the paper. Special thanks are due to Enes Türk, Mehmet Firat and Hasan Hüseyin Duru for their support during the field sessions.

References

Abdioğlu, E., Arslan, M., Kadir, S., Temizel, İ., 2015. Alteration mineralogy, lithochemistry and stable isotope geochemistry of the Murgul (Artvin, Ne Turkey) volcanic hosted massive sulfide deposit: implications to alteration age and ore forming fluids. Ore Geol. Rev. 66, 219–242.

Akaryalı, E., 2010. Arzular (Gümüşhane KD-Türkiye) Altın Yatağının Jeolojik, Mineralojik, Jeokimyasal ve Kökensel İncelenmesi (PhD Thesis) KTÜ, FBE, (174 pp.).

Akaryalı, E., Tüysüz, N., 2013. The genesis of the slab window-related Arzular low-sulfidation epithermal gold mineralization (Eastern Pontides, NE Turkey). Geosci. Front. 4-4, 409–421.

Aslan, N., 2011. Mastra (Gümüşhane) Yatağı'nın Jeolojik, mineralojik ve Jeokimyasal Özellikleri. (Master Thesis) KTÜ, FBE, (190 pp.).

Barton, P.B., Skinner, B.J., 1979. Sulfide mineral stabilities. In: Barnes, H.L. (Ed.), Geochemistry of Hydrothermal Ore Deposits. Wiley Inter Science, New York, pp. 278–403.

Bektaş, O., Yılmaz, C., Taslı, K., Akdağ, K., Özgür, S., 1995. Cretaceous rifting of the eastern Pontide carbonate platform (NE Turkey): the formation of carbonates breccias and turbidites as evidences of a drowned platform. Geologia 57 (1-2), 233–244.

Bektaş, O., Şen, C., Atıcı, Y., Köprübaşı, N., 1999. Migration of the Upper Cretaceous subduction-related volcanism toward the back-arc basin of the eastern Pontide magmatic arc (NE Turkey). Geol. J. 34, 95–106.

Bodnar, R.J., 1993. Revised equation and table for determining the freezing point depression of H_2O–NaCl solutions. Geochim. Cosmochim. Acta 57, 683–684.

Bozkaya, G., Gökçe, A., 2003. Stable isotope (S, O and H) studies at the lead–zinc deposits in the İnler Yaylası (Şebinkarahisar–Giresun), Northeastern Turkey. Bulletin of Earth Sciences Application and Research Centre of Hacettepe University 27, pp. 75–84.

Browne, P.R.L., Lowering, J.F., 1973. Composition of sphalerites from the Broadlands geothermal field and their significance to sphalerite geothermometry and geobarometry. Econ. Geol. 68, 381–387.

Burnham, C.W., Ohmoto, H., 1980. Late-stage processes of felsic magmatism. Min. Geol. Spec. Issue 8, 1–12.

Çiftçi, E., 2000. Mineralogy, Paragenetic Sequence, Geochemistry and Genesis of the Gold and Silver Bearing Upper Cretaceous Mineral Deposits, North Eastern Turkey (Ph. D Thesis, University of Missouri-Rolla, Missouri).

Clayton, R.N., Mayeda, T.K., 1963. The use of bromine penta fluoride in the extraction of oxygen from oxides and silicates for isotopic analysis. Geochim. Cosmochim. Acta 27, 43–52.

Cooke, D.R., Simmons, S.F., 2000. Characteristics and genesis of epithermal gold deposit. In: Hageman, G.S., Brown, E. (Eds.), Gold in 2000. Reviews in Economic Geology 13, pp. 221–241.

Demir, Y., 2005. Istala ve Köstere (Zigana/Gümüşhane) Cu–Pb–Zn Madenleri ve Yan Kayaçlarının Mineralojisi ve Dokusal Özelliklerinin Karşılaştırılmalı İncelenmesi (Master Thesis) KTÜ, FBE, (110 pp.).

Demir, Y., Uysal, İ., Sadıklar, M.B., 2013. Mineral chemical investigation on sulfide mineralization of the Istala deposit, Gümüşhane, NE-Turkey. Ore Geol. Rev. 53, 306–317.

Demir, Y., Uysal, I., Sadıklar, M.B., Ceriani, A., Hanilçi, N., Müller, D., 2015. Mineralogy, mineral chemistry, fluid inclusion, and stable isotope investigations of the Kabadüz ore veins, Ordu, NE-Turkey. Ore Geol. Rev. 66, 82–98.

Demir, Y., Uysal, I., Sadıklar, M.B., Sipahi, F., 2008. Mineralogy, mineral chemistry, and fluid inclusion investigation of Köstere hydrothermal vein-type deposit (Gümüşhane, NE-Turkey. Neues Jb. Mineral. 185 (2), 215–232.

Dewey, J.F., Pitman, W.C., Ryan, W.B.F., Bonnin, J., 1973. Plate tectonics and evolution of the Alpine system. Geol. Soc. Am. Bull. 84, 3137–3180.

Dokuz, A., 2011. A salb detachment and delamination model for the generation of Carboniferous high potassium I-type magmatism in the Eastern Pontides: the Köse composite pluton. Gondwana Res. 19, 926–944.

Eyuboglu, Y., 2010. Late Cretaceous high-K volcanism in the Eastern Pontide Orogenic Belt, and its implications for the geodynamic evolution of NE Turkey. Int. Geol. Rev. 52 (2–3), 142–186.

Eyuboglu, Y., 2015. Petrogenesis and U–Pb zircon chronology of felsic tuffs interbedded with turbidites (Eastern Pontides Orogenic Belt, NE Turkey): implications for Mesozoic geodynamic evolution of the eastern Mediterranean region and accumulation rates of turbidite sequences. Lithos 212-215, 74–92.

Eyuboglu, Y., Bektaş, O., Pul, D., 2007. Mid-Cretaceous olistostromal ophiolitic melange developed in the back-arc basin of the eastern Pontide magmatic arc (NE Turkey). Int. Geol. Rev. 49, 1103–1126.

Eyuboglu, Y., Bektaş, O., Seren, A., Nafiz, M., Jacoby, W.R., Özer, R., 2006. Three-directional extensional deformation and formation of the Liassic rift basins in the Eastern Pontides (NE Turkey). Geol. Carpath. 57 (5), 337–346.

Eyuboglu, Y., Chung, S.L., Santosh, M., Dudas, F.O., Akaryali, E., 2011a. Transition from shoshonitic to adakitic magmatism in the Eastern Pontides, NE Turkey: implications for slab window melting. Gondwana Res. 19, 413–429.

Eyuboglu, Y., Dilek, Y., Bozkurt, E., Bektaş, O., Rojay, B., Şen, C., 2010. Geochemistry and geochronology of a reversely-zoned, Alaskan-type ultramafic–mafic complex in the Eastern Pontides, NE Turkey. In: Santosh, M., Maruyama, S. (Eds.), A Tribute to Akiho Miyashiro. Gondwana Research 18, pp. 230–252.

Eyuboglu, Y., Dudas, F.O., Santosh, M., Xiao, Y., Yi, K., Chatterjee, N., Wu, F.Y., Bektaş, O., 2015b. Where are the remnants of a Jurassic Ocean in the Eastern Mediterranean Region? Gondwana Res. http://dx.doi.org/10.1016/j.gr.2015.08.017.

Eyuboglu, Y., Dudas, F.O., Santosh, M., Yi, K., Kwon, S., Akaryali, E., 2013b. Petrogenesis and U–Pb zircon chronology of adakitic porphyries within the Kop ultramafic massif (Eastern Pontides Orogenic Belt, NE Turkey). Gondwana Res. 24, 742–766.

Eyuboglu, Y., Dudas, F.O., Santosh, M., Zhu, D.C., Yi, K., Chatterjee, N., Jeong, Y.J., Akaryalı, E., Liu, Z., 2015a. Cenozoic forearc gabbros from the northern zone of the Eastern Pontides Orogenic Belt, NE Turkey: Implications for slab window magmatism and convergent margin tectonics. Gondwana Res. http://dx.doi.org/10.1016/j.gr.2015.07.006.

Eyuboglu, Y., Santosh, M., Chung, S.L., 2011c. Petrochemistry and U–Pb ages of adakitic intrusions from the Pulur massif (Eastern Pontides, NE Turkey): implications for slab roll-back and ridge subduction associated with Cenozoic convergent tectonics in eastern Mediterranean. J. Geol. 119, 394–417.

Eyuboglu, Y., Santosh, M., Dudas, F.O., Akaryali, E., Chung, S.L., Akdag, K., Bektas, O., 2013a. The nature of transition from adakitic to non-adakitic magmatism in a slab-window setting: a synthesis from the eastern Pontides, NE Turkey. Geosci. Front. 4, 353–375.

Eyuboglu, Y., Santosh, M., Dudas, F.O., Chung, S.L., Akaryali, E., 2011b. Migrating magmatism in a continental arc: geodynamics of the Eastern Mediterranean revisited. J. Geodyn. 52, 2–15.

Eyuboglu, Y., Santosh, M., Yi, K., Tuysuz, N., Korkmaz, S., Akaryalı, E., Dudas, F.O., Bektas, O., 2014. The Eastern Black Sea-type volcanogenic massive sulfide deposits: geochemistry, zircon U–Pb geochronology and an overview of the geodynamics of ore genesis. Ore Geol. Rev. 59, 29–54.

Field, C.W., Fifarek, R.H., 1985. Light isotope sytematics in the epithermal environment. In: Berger, B.R., Bekte, P.M. (Eds.), Geology And Geochemistry of Geothermal Systems. Reviews in Economic Geology 2, pp. 99–128.

Gemmell, J.B., Large, R.R., 1992. Stringer system and alteration zones underlying the Hellyer volcanogenic massive sulfide deposit, Tasmania, Australia. Econ. Geol. 87, 620–649.

Giggenbach, W.F., 1992. Isotopic shifts in water from geothermal and volcanic systems along convergent plate boundaries and their origin. Earth Planet. Sci. Lett. 113, 495–510.

Gökçe, A., Bozkaya, G., 2003. Fluid inclusion and stable isotope characteristics of the Inler Yaylası lead zinc deposits, northern Turkey. Int. Geol. Rev. 45, 1044–1054.

Güven, I.H., 1993. Geological and Metallogenic Map of the Eastern Black Sea Region; 1: 250000 Map. MTA. Trabzon.

Gottesmann, W., Kampe, A., 2007. Zn/Cd ratios in calcsilicate-hosted sphalerite ores at Tumurtijn-ovoo, Mongolia. Chem. Erde 67, 323–328.

Güner, S., Yazıcı, E.N., 2011. Gümüşhane–Bayburt–Trabzon Kıymetli Metal (Au–Ag) ve Baz Metal (Cu–Pb–Zn) Sahaları Envanter Raporları, Trabzon (Unpublished).

Heald, P., Foley, N.K., Hayba, D.O., 1987. Comparative anatomy of volcanic-hosted epithermal deposits: acid sulfate and adularia-sericite types. Econ. Geol. 82, 1–26.

Hedenquist, J.W., Lowenstern, J.B., 1994. The role of magmas in the formation of hydrothermal ore deposit. Nature 370, 519–527.

Hedenquist, J.W., Matsuhisa, Y., Izawa, E., White, N.C., Giggenbach, W.F., Aoki, M., 1994. Geology, geochemistry, and origin of high sulfidation Cu–Au mineralization in the Nansatsu District, Japan. Econ. Geol. 89, 1–30.

Henley, R.W., Ellis, A.J., 1983. Geothermal systems, ancient and modern. Earth-Sci. Rev. 19, 1–50.

Hoefs, J., 1987. Stable Isotope Geochemistry. 3rd edn. Springer, Berlin-Heidelberg-New York (241 pp.).

Karsli, O., Chen, B., Aydın, F., Şen, C., 2007. Geochemical and Sr–Nd–Pb isotopic compositions of the Eocene Dölek and Sarıçiçek Plutons, Eastern Turkey: implications for magma interaction in the genesis of high-K calc-alkaline granitoids in a post-collision extensional setting. Lithos 98, 67–96.

Karslı, O., Dokuz, A., Uysal, I., Aydın, F., Kandemir, R., Wijbrans, R.J., 2010. Generation of the early Cenozoic adakitic volcanism by partial melting of mafic lower crust, Eastern Turkey: implications for crustal thickening to delamination. Lithos 114, 109–120.

Kaygusuz, A., Aydınçakır, E., 2011. Petrogenesis of a Late Cretaceous composite pluton from the eastern Pontides: the Dagbasi pluton, NE Turkey. Neues Jb. Mineral. Abh. 188, 211–233.

Kaygusuz, A., Arslan, M., Siebel, W., Sipahi, F., Ilbeyli, N., Temizel, I., 2014. LA-ICP MS zircon dating, whole-rock and Sr–Nd–Pb–O isotope geochemistry of the Camiboğazı pluton, Eastern Pontides, NE Turkey: implications for lithospheric mantle and lower crustal sources in arc-related I-type magmatism. Lithos 192-195, 271–290.

Kaygusuz, A., Wolfgang, S., Şen, C., Satir, M., 2008. Petrochemistry and petrology of I-type granitoids in an arc setting: the composite Torul pluton, Eastern Pontides, NE Turkey. Int. J. Earth Sci. 97, 739–764.

Knight, C.L., Bodnar, R.J., 1989. Synthetic fluid inclusions: IX. Critical PVTX properties of NaCl–H_2O solutions. Geochim. Cosmochim. Acta 53, 3–8.

Kudun-Yozgat, K., 2009. Çetilli (Gölköy-Ordu) Yöresinin jeolojisi, jeokimyası ve hidrotermal damar tip cevherleşmeler açısından incelenmesi (Master Thesis) KTÜ, FBE, (132 pp.).

Lermi, A., 2003. Midi (Karamustafa/Gümüşhane, KD Türkiye) Zn-Pb Yatağının Jeolojik, Mineralojik, Jeokimyasal ve Kökensel İncelemesi (PhD Thesis) KTÜ, FBE (321 pp.).

Matsuhisa, Y., Aoki, M., 1994. Temperature and oxygen isotope variations during formation of the Hishikari epithermal gold–silver veins, southern Kyushu, Japan. Econ. Geol. 89, 1608–1613.

Ohmoto, H., 1972. Systematics of sulfur and carbon in hydrothermal ore deposits. Econ. Geol. 67, 551–579.

Ohmoto, H., 1986. Stable isotope geochemistry of ore deposits. In: Valley, J.W., Taylor, H.P., O'nein, J.R. (Eds.), Stable Isotopes in High Temperature Geological Processes. Reviews in Mineralogy Mineralogical Society of America 16, pp. 491–560.

Ohmoto, H., Rye, R.O., 1979. Isotopes sulfur and carbon. In: Barnes, H.L. (Ed.), Geochemistry of Hydrothermal Ore Deposits, Second Edition John Wiley and Sons Inc., New York, pp. 509–567.

O'Neil, J.R., Taylor, B.E., 1969. Oxygen isotope fractionation between muscovite and water. J. Geophys. Res. 74, 6012–6022.

Ransome, F.L., 1907. The association of alunite with gold in the Goldfield District, Nevada. Econ. Geol. 2, 667–692.

Roedder, E., 1984. Fluid Inclusions: Reviews in Mineralogy v. 12. Mineralogical Society of America, Washington, p. 644.
Roedder, E., Bodnar, R.J., 1980. Geologic pressure determinations from fluid inclusion studies. Annu. Rev. Earth Planet. Sci. 8, 263–301.
Scott, S.D., Barnes, H.L., 1971. Sphalerite geothermometry and geobarometry. Econ. Geol. 66, 653–669.
Şengör, A.M.C., Yılmaz, Y., 1981. Tethyan evolution of Turkey: a plate tectonic approach. Tectonophysics 75, 181–241.
Shepherd, T.J., Rankin, A.N., Alderton, D.H.M., 1985. A Practical Guide to Fluid Inclusion Studies. Blacie & Son Press, London (238 s).
Sipahi, F., 2011. Formation of skarns at Gümüşhane (northeastern Turkey). Neues Jb. Mineral. Abh. 188 (2), 169–190.
Sipahi, F., Sadıklar, M.B., Şen, C., 2014. The geochemical and Sr–Nd isotopic characteristics of Murgul (Artvin) volcanics in the eastern Black Sea Region (NE Turkey). Chem. Erde-Geochem. 74, 331–342.
Song, X., 1984. Minor elements and ore genesis of the Fankou lead–zinc deposit, China. Mineral. Deposita 19, 95–104.
Steele-MacInnis, M., Lecumberri-Sanchez, P., Bodnar, R.J., 2012. HOKIEFLINCS_H_2O-NACL: a Microsoft Excel spreadsheet for interpreting microthermometric data from fluid inclusions based on the PVTX properties of H_2O–$NaCl_2$. Comput. Geosci. 49, 334–337.
Taylor, H.P., 1974. The application of oxygen and hydrogen isotope studies to problems of hydrothermal alteration and ore deposition. Econ. Geol. 69, 843–883.
Tayyar, H., 2005. Mastra (Gümüşhane) Epitermal Altın Yatağının Jeolojik ve Jeokimyasal Özellikleri (Master Thesis), CU, FBE, (46 pp.).
Tokel, S., 1972. Stratigraphical and Volcanic History of the Gümüshane Region (NE Turkey) (PhD Thesis, University of College, London).
Topuz, G., Altherr, R., Schwarz, W.-H., Dokuz, A., Meyer, H.-P., 2007. Variscan amphibolite-facies metamorphic rocks from the Kurtoğlu metamorphic complex (Gümüşhane area, Eastern Pontides, Turkey). Int. J. Earth Sci. 96, 861–873.
Topuz, G., Altherr, R., Schwarz, W.H., Siebel, W., Satir, M., Dokuz, A., 2005. Post-collisional plutonism with adakite-like signatures: the Eocene Saraycik granodiorite (Eastern Pontides, Turkey). Contrib. Mineral. Petrol. 150, 441–455.
Topuz, G., Altherr, R., Wolfgang, S., Schwarz, W.H., Zack, T., Hasanözbek, A., Mathias, B., Satır, M., Şen, C., 2010. Carboniferous high-potassium I-type granitoid magmatism in the Eastern Pontides: the Gümüşhane pluton (NE Turkey). Lithos 116, 92–110.
Tüysüz, N., 2000. Geology, lithogeochemistry and genesis of the murgul massive sulfide deposit, NE Turkey. Chem. Erde 60, 231–250.
Tüysüz, N., Akçay, M., 2000. Doğu Karadeniz Bölgesindeki Altın Yataklarının Karşılaştırmalı İncelemesi. Cumhuriyetin 75. Yılı Yer Bilimleri ve Madencilik Kongresi, Ekim, MTA, Ankara, Bildiriler Kitabı, pp. 625–645.
Tüysüz, N., Özdoğan, K., Er, M., Yılmaz, Z., Ağanoğlu, A., 1994. Pontid Adayayında Carlin Tipi Kaletaş (Gümüşhane) Altın Zuhuru. Türk. Jeol. Bül. 37, 41–46.
Ueda, A., Krouse, H.R., 1986. Direct conversion of sulphide and sulphate minerals to SO_2 for isotope analysis. Geochem. J. 20, 209–212.
White, N.C., Hedenquist, J.W., 1990. Epithermal environments and styles of mineralization: variations and their causes, and guidelines for exploration. J. Geochem. Explor. 36, 445–474.
Wilkinson, J.J., 2001. Fluid inclusions in hydrothermal ore deposits. Lithos 55, 229–272.
Yalçınalp, B., 1992. Güzelyayla (Maçka–Trabzon) Porfiri Cu–Mo Cevherleşmesinin Jeolojik Yerleşimi ve Jeokimyası (PhD Thesis), KTÜ, FBE, (175 pp.).
Yaylalı-Abanuz, G., Tüysüz, N., 2010. Chemical, mineralogical, and mass-change examinations across a gold bearing vein zone in the Akoluk area, Ordu, NE Turkey. Neues Jb. Mineral. 187 (1), 11–22.